2018

A stratigraphic and microfossil record of coseismic land-level changes and tsunami deposits from Old Harbor, Central Kodiak Island, Alaska

Greta Janigian
University of Rhode Island, gjanigian@uri.edu

A STRATIGRAPHIC AND MICROFOSSIL RECORD OF COSEISMIC LAND-LEVEL CHANGES AND TSUNAMI DEPOSITS FROM OLD HARBOR, CENTRAL KODIAK ISLAND, ALASKA

BY

GRETA JANIGIAN

A THESIS SUBMITTED IN PARTIAL FULFILLMENT OF THE

REQUIREMENTS FOR THE DEGREE OF

MASTER OF SCIENCE

IN

BIOLOGICAL AND ENVIRONMENTAL SCIENCE

UNIVERSITY OF RHODE ISLAND

2018

MASTER OF SCIENCE IN BIOLOGICAL AND ENVIRONMENTAL SCIENCE

OF

GRETA JANIGIAN

APPROVED:

Thesis Committee:

Major Professor Simon Engelhart

Brian Savage

John King

Tina Dura

Nasser H. Zawia
DEAN OF THE GRADUATE SCHOOL

UNIVERSITY OF RHODE ISLAND
2018

ABSTRACT

To reconstruct the paleoseismic history of Old Harbor on Kodiak Island, Alaska, we undertook exploratory coring at two coastal sites, Big Creek and Bear Terrace, 4 km and 2 km northeast of Old Harbor, respectively. We chose the longest core from Big Creek for analysis (90 cm, BC.15.02). Six sand to sandy-silt layers deposited within organic silts and peats occur in this core. Radiocarbon dating, a tephra deposit, and radiometric marker (^{137}Cs) analyses were used to estimate ages of sand and silt deposition. ^{137}Cs results confirmed that the uppermost clastic deposit records the AD 1964 Great Alaskan earthquake and tsunami, the most recent large tsunami to inundate Old Harbor. This clastic layer lies 3 cm above a layer of pumice from the AD 1912 eruption of Mount Katmai, which is located ~150 km northwest of Old Harbor. We were able to use the characteristics of the AD 1964 tsunami deposit (thick, coarse-grained, normally graded sequences, increase in marine and epipsammic diatoms) as a guide for identifying tsunami deposits in the rest of the core. Lithologic, diatom, grain-size, and statistical analyses pointed out characteristics specific to tsunami deposits, helping us to differentiate between the five deeper clastic deposits in the core. We identified the bottommost clastic deposit as a tsunami deposit from the AD 1788 earthquake. Both the AD 1964 and AD 1788 deposits in our core contained the characteristic features of tsunami deposits, but there was little indication of land level change associated with either deposit, which contrasts with observations and previous studies. Detrended correspondence analysis (DCA) on our diatom assemblages identified the difference between the local tsunami deposits and clastic deposits from other depositional

mechanisms. Therefore, we inferred that the other four clastic deposits were most likely deposited by floods, storms, or tele-seismic tsunamis.

ACKNOWLEDGMENTS

I would like to thank, above all, my graduate advisor, Dr. Simon Engelhart, for his immense support and guidance throughout my time as a student. I admire your strong work ethic and have learned so much from you these past two years. I truly appreciate the opportunity to work with you and the opportunities you have given me. I also owe a huge thank you to Dr. Tina Dura who helped me conquer diatoms. I feel honored to have learned from the diatom queen. Thank you to my other committee members, Dr. Brian Savage, who is always so encouraging, Dr. John King, and Dr. Rebecca Robinson, for chairing my defense.

I am also incredibly lucky to have worked with such intelligent and supportive lab mates; thank you Rachel Stearns, J Padgett, Byron Halavik, Dan Russell, and Nicole Brennan for all of your help in and out of the lab. And thanks to Michaela Cashman for being a first-rate officemate. Lastly, I would like to thank my parents, Leo, Lily, and Medzmama for all of the love and support.

PREFACE

This thesis is written in manuscript format in accordance with the requirements of the Graduate School of the University of Rhode Island. This thesis contains one manuscript and one appendix. The thesis, entitled A stratigraphic and microfossil record of coseismic land-level changes and tsunami deposits from Old Harbor, Central Kodiak Island, Alaska, is prepared for submission to the journal *OpenQuaternary*.

TABLE OF CONTENTS

LIST OF TABLES

LIST OF FIGURES

Manuscript 1

A stratigraphic and microfossil record of coseismic land-level changes and tsunami deposits from Old Harbor, Central Kodiak Island, Alaska

Janigian, G.[1], Engelhart, S.E.[1], Dura, T.[2], Witter R.C.[3], Briggs, R.W.[4], Koehler, R.D.[5], Padgett, J.S.[1], Corbett, D.R.[6]

is prepared for submission to the journal *OpenQuaternary*

---

[1]Department of Geosciences, University of Rhode Island, Kingston, Rhode Island 02882 USA
[2]Department of Geology, Humboldt State University, Arcata, California 95521 USA
[3]Alaska Science Center, U.S. Geological Survey, Anchorage, Alaska 99508 USA
[4]Geologic Hazards Science Center, U.S. Geological Survey, Golden, Colorado, USA
[5] Nevada Bureau of Mine and Geology, Mackay School of Earth Sciences and Engineering, University of Nevada, Reno, USA
[6]Department of Geological Sciences, UNC Coastal Studies Institute, North Carolina 27981, USA

1. Introduction

The Alaska-Aleutian subduction zone is one of the most seismically active subduction zones in the world (United States Geological Survey, 2014). Almost the entire subduction zone interface ruptured in the 20th century with seven earthquakes greater than M8.0 in 1987, 1965, 1964, 1957, 1946, 1938, and 1906. The largest of these was the M9.2 1964 earthquake, rupturing the eastern segments of the subduction zone (Carver and Plafker, 2008; Plafker 1969). The subsequent tsunami caused severe damage to many coastal towns in Alaska. Various tsunami modeling scenarios have predicted that large earthquakes along the subduction zone have the potential to create tsunamis strong enough to impact coastal California and Hawaii (Butler, 2012; Butler et al., 2017; Ryan et al., 2011; Kirby et al., 2012). However, the instrumental record of earthquakes along the Alaska-Aleutian subduction zone only dates back to the early 1900s. Therefore, in order to learn more about historic and prehistoric earthquakes before the installation of seismometers along the Alaska-Aleutian megathrust, we employ paleoseismology methods to investigate the record of earthquakes and tsunamis recorded in the sediments along the subduction zone. Our results will help better assess seismic hazards in the region and inform future scientific investigations in the area.

Subduction zone paleoseismology employs coastal stratigraphy and micropaleontology to document signs of past earthquakes and tsunamis, allowing us to extend the seismic record beyond the historical and instrumental period. Coseismic land-level change and tsunami inundation leave distinct signatures in the lithology and grain size of coastal sediments (e.g., sudden switches in sediment type, sand/silt deposits) that

differ from sediments from the interseismic period (Nelson et al., 1996; Dura et al., 2016). Microfossils such as diatoms can provide an independent test of coseismic land-level change and tsunami inundation inferred from coastal sediments because of their sensitivity to environmental factors including salinity, tidal exposure, and substrate (Hemphill-Haley, 1995a; Shennan et al., 1999; Sawai, 2001; Shennan and Hamilton, 2006). The utility of diatoms as indicators of coastal environmental change also stems from the high preservation potential of their siliceous valves in coastal sedimentary archives (Hamilton et al., 2005; Sawai et al., 2008). However, one complication of paleoseismology is differentiating between tsunami deposits and clastic sediments deposited by other mechanisms, since their characteristics can be similar (Switzer and Jones, 2008; Morton et al., 2007; Kortekaas and Dawson, 2007).

Paleosesimology studies have been conducted along subduction zones all over the world in Chile (Dura et al., 2015b; Hong et al., 2016), U.S. Pacific Northwest (Hemphill-Haley, 1995; Witter et al., 2003), and Japan (Sawai et al. 2008; Nanayama et al., 2007). Previous paleoseismic studies in Alaska have looked at sediments in the general region of the AD 1964 rupture zone to infer rupture and tsunami inundation extent, and to look for evidence of historic and prehistoric earthquakes and tsunamis (Figure 1; Shennan et al., 2014; Briggs et al., 2014; Nelson et al., 2015; Shennan et al., 2013; Shennan et al., 2005; Shennan et al., 1999; Shennan et al., 2009; Shennan et al., 2014b; Hamilton et al. 2004a; Hamilton et al., 2004b; Combellick, 1994). The AD 1964 rupture boundary is fairly well constrained, but questions still remain about the rupture patterns and tsunami extents of past great earthquakes in the Kodiak Island region.

We investigated marsh deposits from central Kodiak Island (Figure 2) for stratigraphic and microfossil evidence of historic and prehistoric earthquakes and tsunamis. We aimed to answer three main research questions: 1) Is the lithological evidence of paleoearthquakes (land-level changes and/or tsunami deposits) at Old Harbor comparable with other records from nearby sites to the north and south? 2) Is there evidence for the AD 1788 earthquake at Old Harbor? 3) Can diatoms and/or grain-size data aid in identifying whether or not clastic layers are deposited by tsunami? To address these questions, we performed a complete lithologic, grain-size, and diatom analysis on a sediment core collected from Big Creek marsh in Old Harbor on Kodiak Island (Figure 2). We developed a composite chronology for the core so we could constrain the timing of the events and compare them to the existing paleoseismic records from nearby sites. We found a total of six clastic deposits in the stratigraphic record from Central Kodiak Island dating back to the mid 1700s. Using the stratigraphic, diatom, sedimentological, dating, and statistical analyses, we identified two of these clastic deposits as tsunami sands from past megathrust earthquakes along the Alaska-Aleutian subduction zone (AD 1964 and AD 1788), which matched findings from previous studies. However, we did not see signs of significant land-level changes associated with the events, disagreeing with some studies from nearby sites. We concluded that the other four clastic deposits were most likely deposited by floods, storms, or tele-seismic earthquakes.

2. Study Area

The Alaska-Aleutian subduction zone is a ~3000 km long megathrust boundary, where the Pacific plate is subducting beneath the North American plate at ~54-78 mm/yr (~60 mm/yr near Central Kodiak Island; Figure 1; Carver and Plafker, 2008). The subduction zone has been divided into 17 segments, based on the rupture extents of past earthquakes (Nishenko and Jacob, 1990). Four successive segments of the subduction zone (Kodiak Island, Prince William Sound, Alaska Peninsula, and Yakataga-Yakutat) ruptured during the AD 1964 earthquake (Carver and Plafker, 2008; Plafker, 1969). Our study site, Old Harbor on Kodiak Island (Figure 2a&b), is at the western end of the AD 1964 rupture zone and lies near the border of subsidence and uplift caused by the AD 1964 rupture (Figure 1). Old Harbor was severely damaged both by subsidence and a tsunami with a run-up of 7.3 m above Mean Sea Level (Kachadoorian and Plafker, 1967). Thirty-four of 35 residences were destroyed (Khachadoorian and Plafker, 1967). Plafker and Kachadoorian (1966) estimated coastal subsidence at 0.6-0.9 m, which may include a component of compaction of the coastal sediments. Old Harbor likely lies within the rupture area of an earthquake in AD 1788 that was reported 15 km to the southwest at Three Saints Bay (Figure 1 & 2a; Soloviev, 1990) and found in the sediment record at a site in northern Kodiak (Shennan, 2014). Old Harbor is also within the proposed rupture area of a prehistoric earthquake that previous paleoseismic studies date to approximately 500 yBP (Figure 1; Gilpin, 1995; Briggs et al., 2014; Shennan et al., 2014).

Kodiak Island, Alaska (Figure 2a) is an island ~40 km southeast of the mainland of Alaska separated by the Shelikof Strait. Kodiak Island is made up of Mezozoic and

Tertiary marine sedimentary rocks and some volcanic rocks in the Old Harbor region (Plafker and Kachadoorian, 1966). The central region of Kodiak Island, where Old Harbor (Figure 2b) is located, is mountainous and the coastline is rocky and steep, with many narrow inlets and islets (Plafker and Kachadoorian, 1966; Capps, 1934). Some areas of Kodiak are also covered in a thin layer of unconsolidated sediments from glacial, alluvial, delta, and beach deposits, this includes part of Old Harbor (Plafker and Kachadoorian, 1966; Capps, 1934). The primary salt marsh plants on Kodiak Island are *Carex*, *Puccinella phryganodes, Triglochin maritima, Triglochin palustris, Puccinella triflora, and Potentilla egedii* (Gilpin, 1995).

The southern Alaska shelf, including Kodiak Island, is affected by glacio-isostatic adjustment from the removal of the Cordilleran ice sheet at the end of the last glacial period. Kodiak is in the region that has been reported to be subsiding around 0.5 mm/yr (Gilpin, 1995). The tide gauge that has been in place on Kodiak since AD 1950 recorded ~1 mm/yr of relative sea-level rise (RSL) prior to AD 1964 (NOAA). The tide gauge was reinstalled in AD 1975 after being destroyed by the AD 1964 earthquake, and since then RSL has been falling ~9.99 mm/yr (NOAA), due to postseismic land uplift after the sudden coseismic subsidence.

The two specific sites from which sediment samples for this study were collected, Big Creek (Figure 2c) and Bear Terrace (Figure 2d), are salt marshes in Old Harbor, both near river mouths in tidally influenced inlets. The diurnal tidal range in the area of Old Harbor is 2.68 m (NOAA). The Big Creek marsh lies along many winding stream channels, which are prone to flooding. At Bear Terrace tidal inundation is limited by flow

through a culvert because of the emplacement of a road nearby. Big Creek had the deepest sediment record with the most sand and silt deposits present within its stratigraphy.

3. Methods

3.1 Sediment coring

We described eleven sediment cores at Big Creek and seven at Bear Terrace to determine the extent of sand and silt deposits within the peat (Figure 2c&d). We described the stratigraphy of the cores using the Troels-Smith classification system (1955; Nelson et al., 1996) to distinguish between sand, silt, and peat deposits. We also analyzed the sharpness of the contacts between the different layers and looked for other features typical of tsunami deposits (Nelson et al., 1996). We collected cores at various points along the littoral zones that contained the deepest records of clastic deposits and we chose the longest core, BC.15.02, for primary analyses. We collected the cores in overlapping 50 cm segments using a Russian corer to ensure proper core recovery and to prevent compaction during the coring process and sample contamination. To preserve the cores, we transferred them to PVC tubes, wrapped them in plastic, and stored them at 4°C.

3.2 Field surveying

We surveyed salt marshes at both Bear Terrace and Big Creek. Our field goal was to find suitable coring locations with long sediment records holding archives of past earthquake events. We used a real-time kinematic (RTK) GPS using a base and rover to determine the precise locations (precision of <0.01 m) and elevations (precision of <0.04 m) of each sample location and tied them to local tidal datums by surveying to the tide

gauge at Old Harbor (NOAA ID: 9457527), ~2 km from Bear Terrace and ~4 km from Big Creek.

3.3 Computerized tomography and X-ray images

Computerized tomography (CT) scans were taken of all the cores at South County Hospital in Rhode Island. The CT machines take cross sectional images of the core and measure the radiodensity of the material in Houndsfield units. The CT images were analyzed using Horos computer software; denser areas are signified by warmer colors. X-ray images were also taken of all cores at University of Rhode Island Health Services to view density differences within the cores. In the X-ray images, denser areas are signified by lighter colors. The CT and X-ray images helped to identify density changes and sharpness between units that are not obvious from optical inspection (Briggs et al., 2014; Nelson et al., 2015).

3.4 Chronology

We developed a chronology for our cores by using radiocarbon (^{14}C), radiometric (^{137}Cs), and tephra methods. ^{137}Cs was particularly important for our cores since the peak of cesium in the atmosphere occurred in AD 1963 after the Limited Test Ban Treaty, just before the AD 1964 earthquake. Our cores also have a layer of pumice from the AD 1912 eruption of the Katmai volcano, just northwest of Kodiak Island. This pumice layer acts as a relative age marker in this section of our core.

When using radiocarbon dating, material younger than ~1600 CE yields multiple calibrated age ranges because of a plateau in the calibration curve (Stuiver and Pearson, 1993). Thus, we sampled the upper 40 cm of core BC.15.02 in one-cm increments for ^{137}Cs activity analysis. The samples were dried at ~40°C, ground to a powder with a mortar and pestle, placed in plastic vials, and shipped to Dr. Reide Corbett at UNC Coastal Studies Institute to measure ^{137}Cs activity by direct gamma counting (Corbett et al., 2009). We extracted in-situ plant macrofossils (rhizomes) from the core from directly above and below lithologic contacts for radiocarbon dating beginning at 42 cm. The material was cleaned, dried at ~40°C, weighed, and sent to National Ocean Sciences Accelerator Mass Spectrometry (NOSAMS) facility at Woods Hole Oceanographic Institution (WHOI) for acid-base-acid pretreatment and accelerator mass spectrometry (AMS) radiocarbon dating.

We produced a Bayesian age-depth model using Bchron (Haslett and Parnell, 2008; Parnell et al., 2011) to produce a composite chronology for core BC.15.02. We assigned normal probability distributions to the ^{137}Cs and tephra age markers. We calibrated the radiocarbon dates using the IntCal13 dates (Reimer et al., 2013) to obtain 2σ (95%) probability age ranges. In our model, we removed the clastic deposits and adjusted the inputted depths since we know these units were deposited instantaneously and may distort the model (Parnell and Gehrels, 2015). Bchron created a chronology for the entire core and we used this age model to estimate the timing of sand and silt deposition. With our completed chronology, we were able to compare ours to nearby chronologies and try to associate clastic layers with known earthquake and tsunami

events. We also looked at the maximum calibrated radiocarbon ages to assess the reliability of the age model.

3.5 Grain Size

We measured the grain size of sediment samples from core BC.15.02 using a Malvern Mastersizer 3000 laser particle size analyzer. The cores were sampled every cm through each clastic bed, as well as 3 cm above and below each clastic unit. The samples were treated with 30% hydrogen peroxide to dissolve any organic material and the remaining inorganic material was analyzed on the Mastersizer (Switzer and Pile, 2015). The d10 (the diameter of which 10% of the grains are smaller) and d50 (50% of grains are smaller) particle size class was mainly used to distinguish grain size between the samples and help distinguish tsunami deposits from other clastic deposits, either from storm, or flood events (Dura et al., 2015; Kortekaas and Dawson, 2007; Morton et al., 2007; Folk, 1966).

3.6 Diatom Analysis

Diatoms work particularly well in our area to test for paleoenvironmental changes because their fossils are typically well preserved in salt marsh sediments and they are quite sensitive to different environmental conditions (Dura et al., 2015; Dawson et al., 1996; Hemphill-Haley, 1996; Zong et al., 2002; Barlow et al., 2012). We use diatoms, instead of foraminifera, for our study in Alaska because salt marsh foraminifera have particularly low species diversity at high latitudes. We completed a diatom analysis

throughout core BC.15.02, which helped in determining sediment provenance (Dawson and Stewart, 2007; Hemphill-Haley, 1995).

We sampled core BC.15.02 in one cm increments for diatom analysis beginning 3 cm above each clastic bed and down to 3 cm below each clastic bed, as well as every 2-3 cm through thick peat sequences. Within the largest clastic layer, samples were taken every 3 cm. The sediment samples were treated with 30% hydrogen peroxide to dissolve any organic material in the sample and then centrifuged and decanted. After the hydrogen peroxide treatment, approximately 25 ml per sample was dripped with a pipette and spread evenly onto a cover slip and left to dry. The dried cover slips were then mounted onto labeled microscope slides using Naphrax and viewed on a Leica microscope under oil immersion and 1000x magnification. At least 300 diatom individuals were counted and identified per sample to species level using reference materials (Diatoms of the United States, 2017). The diatoms were used to infer sediment provenance based on their salinity preferences and life-form using sources including Hemphill-Haley (1993), Krammer and Lange-Bertalot (1986, 1988, 1991a, 1991b), Vos and de Wolf (1988, 1993), and Denys (1991). Salinity preferences were defined as either freshwater, brackish, or marine and life-form was distinguished by either epyphytic (attach to plant/algae), epipelic (attach to clay or silt grains), or epipsammic (attach to sand grains).

Deposits from turbulent, high energy flows, such as tsunamis, sometimes contain a higher percentage of fractured diatom valves than diatoms in other deposits (Dawson et al., 1996; Dawson, 2007; Witter et al., 2009; Nelson et al., 2015). We scanned the diatom

slides at low magnification (400x) to determine the percentage of fractured diatoms. We counted all diatoms larger than 40 μm, counting at least 100 valves per sample.

To further evaluate patterns within the diatom assemblages from our samples, we performed a detrended correspondence analysis (DCA) using the MVSP computer software program (Horton and Edwards, 2006; Dura et al., 2015). We included all diatom species with >2.5% abundance when inputting the data for analysis. Samples made up of similar assemblages are grouped together on the DCA plot and samples that differ are grouped apart.

4. Results

4.1 Stratigraphy

We described the stratigraphy at Big Creek and Bear Terrace using 11 cores and 7 cores, respectively (23-100 cm long). The stratigraphy at both Bear Terrace and Big Creek consists of peat and silty peat with multiple sand and silt beds throughout the peats. All of the cores had an uppermost sand/silt unit (clastic deposit 1) that was most likely deposited by the AD 1964 tsunami (Figure 3). The cores from Big Creek and Bear Terrace both include a tephra layer from the AD 1912 Katmai eruption and multiple sand and silt beds below the first clastic deposit (Figure 3). Our longest core from Big Creek (BC.15.02) had both the greatest number and best representation of clastic units in the top 90 cm. We chose core BC.15.02 for stratigraphic, diatom, grain-size, and chronological analyses (Figure 4).

In core, BC.15.02, organic modern peat is present from the surface down to 14 cm. Directly below the modern peat is a 17 cm thick sand unit that extends from 14-31 cm (clastic deposit 1). The contact between this sand unit and the overlying peat is diffuse (~10 mm), but the contact between this sand and the underlying silty peat unit is sharp and abrupt (~2 mm). The silty peat layer extends from 31 to 36 cm. A thin layer of white pumice from the AD 1912 eruption of Mount Katmai is present within this unit at 34 cm. There is a 2 cm thick sandy silt unit from 36 to 38 cm (clastic deposit 2), which includes some peat within it and has a diffuse upper contact similar to the clastic deposit 1. The contact between this unit and underlying silty peat is fairly sharp (~4 mm) but not

as sharp as the lower boundary of clastic deposit 1. Five cm of silty peat separates this unit from another 2.5 cm sandy silt unit (clastic deposit 3), which extends down to 46.5 cm depth and includes some organic material within it. This unit has a fairly sharp (4 mm) boundary with the overlying peat but a slightly more gradual (~6 mm) lower boundary. Seven cm of silty peat separates clastic deposit 3 and a 3 cm sandy silt deposit (clastic deposit 4). This unit has an abrupt contact (2 mm) with the underlying silty peat but a diffuse boundary (10 mm) with the peat above. A thick sequence of primarily silty peat (~15 cm) lies below clastic deposit 4. There is a sudden switch to a thin sandy silty unit at 69 cm which is only 1.5 cm thick (clastic deposit 5). It has distinct boundaries with the peat above and the thin layer of underlying peat (both contacts ~3 mm). Extending from 71-82 cm is a sand deposit with a straight (clastic deposit 6), very sharp contact with the peat above it (~1 mm). The boundary between this sand and the silty peat below is at an angle but still abrupt (~3 mm). Silty peat continues down to 90 cm until core refusal.

4.2 Grain-size

Clastic deposit 1 is a medium to coarse grained sand with an average d10 grain-size of 32.4 μm and average d50 of 134.6 μm. Grain-size analysis through this sand shows three separate upward fining sequences; one from 30-27 cm, one from 25-18 cm, and one from 16-13 cm at the very top of the clastic unit. The coarsest material is in the middle of clastic deposit 1. The grain-size drops through the peat below clastic deposit 1 and then slightly increases through clastic deposit 2 (average d10: 12.9 μm average d50:

71.9 μm) but remains relatively fine. Clastic deposit 3 (average d10: 9.5 μm; average d50: 43.8 μm) also has a similar grain-size to the peat above and below it, mostly made up of silt grains with a few larger sand grains. The grain-size increases through clastic deposit 4 (average d10: 15.1 μm; average d50: 78.5 μm). There is one particularly coarse layer made up of sand grains with a d10 value 24.2 μm but we could not identify any grading. The grain-size becomes very fine through the peat and then increases to an average d10 of 17.4 μm (average d50: 73.9 μm) through clastic deposit 5. There is a large jump in the grain-size through clastic deposit 6. Similar to clastic deposit 1, clastic deposit 6 contains multiple upward fining sequences, one in the bottom-middle section of the unit (77-75 cm) and one at the top (75-71 cm). The average d10 value through the entire unit is 33.3 μm and d50 is 142.5 μm, but the upper half of the sand (71-75 cm) is much coarser with an average d10 of 51.0 μm and average d50 of 169.8 μm.

4.3 Diatom assemblages

The diatom assemblage in the peat directly above clastic deposit 1 is made up of primarily freshwater diatoms (e.g., *Pinnularia borealis)* and epiphytic and epipelic diatoms (e.g., *Navicula pusilla* and *Navicula capitata*). There is an increase in marine diatoms in the peat between 7 and 9 cm depth (e.g., *Cocconeis scutellum* and *Cocconeis costata*). The diatom assemblage within clastic deposit 1 is a mixed assemblage of freshwater, brackish, and marine species, but shows a significant increase in marine and brackish diatoms (e.g., *Cocconeis costata, Cocconeis scutellum, Navicula phyllepta, Planothidium lanceolatum*) and an even bigger increase in epipsammic diatoms (e.g.,

Planothidium delicatulum), particularly through the coarsest section of the sand (~30% increase). At 32 cm, the diatom assemblage switches back to primarily freshwater species, similar to just above clastic deposit 1.

Clastic deposit 2 also contains a mixed assemblage of freshwater, marine, and brackish diatoms, but the percentage of both marine and brackish diatom species increases by 10-15% from the peat above it. The overall percentage of marine diatoms is not as high as in clastic deposit 1 (average 45% for deposit 1 compared to average 35% for deposit 2). The silty peat below clastic deposit 2 has a high percentage of epipelic (~60%) and freshwater diatoms. (~80%). Around 44 cm, we see a significant increase in epiphytic diatoms (e.g., *Navicula capitata*), from ~35% to 65%). The epiphytic increase continues through clastic deposit 3. The rest of the diatom assemblage of clastic deposit 3 is mixed but increases in marine and brackish, and epipsammic diatoms, compared to the peat above and below it. Instead of the typical freshwater diatom assemblage, the peat above clastic deposit 4 contains a more brackish diatom assemblage (e.g., *Navicula cincta* and *Navicula phyllepta*). This increase begins around 51 cm. Similar to clastic deposits 2 and 3, clastic deposit 4 has a mixed assemblage but increases in marine diatoms by ~15%. It has a slightly more brackish assemblage than the other clastic deposits. The peat in between clastic deposits 4 and 5 contain mainly freshwater, epiphytic, and epipelic diatoms, and some marine diatoms as well.

Clastic deposit 5 contains fewer marine and epipsammic diatoms than the other clastic deposits and has a similar assemblage to the peat surrounding it. Additionally, the dominant brackish and marine diatom species vary from the other clastic deposits. This

deposit contains more of the brackish species *Nitzchia commutata* and fewer *Planothdium lanceolatum*. Clastic deposit 6 contains a similar diatom assemblage to clastic deposit 1, with a significant increase in marine and brackish diatoms, as well as an even more significant increase in epipsammic diatoms particularly through the coarsest sections of the sand. In the peat directly above and below this deposit, the diatom assemblage switches to primarily freshwater (~75%) and epipelic (~60%) diatoms.

The percentage of fractured diatom valves in clastic deposits 1, 2, 3, and 6 all had fracture percentages between 63-65%. The peats above and below these clastic deposits contained an average of 58% fractured valves. Clastic deposits 4 and 5 had slightly lower fracture percentage: 50% and 49%, respectively. The peats above and below these clastic deposits contained ~43% fractured diatom valves.

The DCA statistical analysis of the diatom samples presented three distinct clusters of samples (Figure 5). Samples from clastic deposits 1 and 6 were grouped together with low axis 1 values (0.0-0.5), samples from clastic deposits 2, 3, 4, and 5 had mid-range axis 1 values (0.5-1.5), and samples from peat deposits had the highest axis 1 values (1.5-2.25). Samples from along the lithologic contacts of clastic deposit deposits 1 and 6 had higher axis 1 values (1.25-2.0) and grouped with the peat samples. One outlier sample from clastic deposit 6 plots with the samples from clastic deposits 2, 3, 4, and 5.

4.4 Chronology

Radiocarbon dating of core BC.15.02 reveals that the sediments at the base of core dates back to ~AD 1650. The peak in ^{137}Cs activity in our core falls at 32 cm, just

below clastic deposit 1 (Table 2). The peak is a result of the maximum ^{137}Cs atmospheric fallout in AD 1963 after the Limited Test Ban Treaty (Carter and Moghissi, 1977) and therefore we assigned 32 cm depth an age of AD 1963. At 34 cm, there is a layer of tephra deposited by the AD 1912 eruption of Mount Katmai, which acts as an age marker in our core (Fierstein and Hildreth, 1992). Thus, 34 cm depth was assigned an age of AD 1912. Seven radiocarbon dates from 43 cm down to 87 cm helped to constrain the ages of the lower clastic units. All of our radiocarbon dates produced multiple 95% calibrated age ranges (Table 1; Figure 6)) because their ages fall within the radiocarbon modern plateau (AD 1600-1950; Stuiver and Pearson, 1993).

Our age-depth model for core BC.15.02 estimates times of deposition for each of the clastic deposits below clastic deposit 1, AD 1964 (Figure 7). The modeled depositional ages are: 43-78 yBP (clastic deposit 2), 87-124 yBP (clastic deposit 3), 155-183 yBP (clastic deposit 4), 204-242 yBP (clastic deposit 5), and 239-278 yBP (clastic deposit 6).

5. Discussion

5.1 Identifying tsunami deposits in core BC.15.02

The stratigraphy at Old Harbor indicates that continuous peat deposition has been interrupted six times by clastic deposits over the last ~400 years. These deposits are most likely the result of either local Alaska-Aleutian megathrust tsunamis, storms, floods, or tele-seismic tsunamis.

We have ample evidence that the AD 1964 tsunami completely inundated Old Harbor with tsunami run-up heights of several meters from various eyewitnesses (Plafker, 1969; Plafker and Khachadoorian, 1966). We interpret clastic deposit 1 to be a tsunami sand deposited by the AD 1964 earthquake and tsunami. The ^{137}Cs activity peak, which marks the year AD 1963, immediately below clastic deposit 1 strongly supports this interpretation. The unit is thick and contains a fairly wide range of grain sizes (silt to coarse sand), which are both typical traits of tsunami deposits (Switzer and Jones, 2007; Dawson and Stewart, 2007; Peters et al., 2001). The fining upward sequences we see within clastic deposit 1 are also typical of tsunami deposits; coarser material is deposited as the tsunami initially brings in the large magnitude of water and then finer material is deposited during the "standing" period as wave energy rapidly decreases (Dawson and Stewart, 2007; Kortekaas and Dawson, 2007). Storms tend to bring in smaller amounts of water and deposit sediments more quickly than tsunamis, making it less likely to see grading patterns in the deposits (Switzer and Jones, 2008). The successive normally graded sequences most likely reflect multiple pulses from the tsunami wave (Dawson et al., 1991; Dawson and Stewart, 2007; Fujino et al., 2006). The abrupt contact at the base

of this sand between the peat and sand deposit is also common of extremely high energy waves like a tsunami wave (Bourgeois, 2009; Witter et al., 2003). We also see evidence in our diatom results that validate our interpretation of clastic deposit 1 as the AD 1964 tsunami deposit. Mixed diatom assemblages with an increase in marine and brackish diatoms are typical for tsunami deposits because tsunamis transport and deposit far field sediments but still erode and deposit nearshore sediments as they inundate (Dawson et al., 1996; Dura et al., 2015). The significant increase in marine diatoms (~30%) and relatively large increase in brackish diatoms (15%) is also typical of a tsunami deposit (Hemphill-Haley, 1995; Dawson et al., 1996; Dura et al., 2015). The large increase in epipsammic diatoms, like *Planothidium delicatulum*, also strongly indicates a marine source for the sands, as we see very few (~10%) epipsammics in the peat.

We used the lithologic and microfossil characteristics of clastic deposit 1 as a guide for the other sand/silt deposits in the core (Table 3). Using those lines of evidence, we interpret clastic deposit 6 to be a tsunami deposit; most likely from the AD 1788 earthquake and tsunami, as the core is too young to record the 500 yBP earthquake (e.g., Gilpin, 1995; Briggs et al., 2014; Shennan et al., 2014). Reports from Russian settlers state that Three Saints Bay, 15 km west of Old Harbor, was hit by a large earthquake (estimated M8) in the summer of AD 1788 (Soloviev, 1990). The grain-size of clastic deposit 6 (average d50: 134.6 μm) follows similar patterns to those of clastic deposit 1 (average d50: 142.5 μm). Like deposit 1, deposit 6 is thick (11 cm) and predominantly composed of fine sand but includes a range of grain-sizes (silt to medium sand). It contains multiple fining upwards sequences, again suggesting successive tsunami waves

with multiple periods of standing water (Dawson et al., 1991; Dawson and Stewart, 2007; Fujino et al., 2006). The irregular, angled contact between the underlying peat and deposit 6 suggest erosion took place during the time of deposition. Erosional contacts are a common feature of tsunami deposits because of their sudden, strong impact energy (Dawson and Stewart, 2007; Fujino et al., 2006; Nelson et al., 2015). In addition, the duplicate core from this location includes a rip-up clast in the top of the sand unit, a feature common to tsunami deposits (Dawson et al., 1991; Kortekaas and Dawson, 2007; Morton et al., 2007). The diatom assemblage of clastic deposit 6 is similar to deposit 1, dominated by the same epipsammic diatom species and increasing by ~25% in marine diatoms from the peat above and below. Additionally, the samples from clastic deposits 1 and 6 cluster together and apart from the rest of the clastic deposits on the DCA plot, indicating that these two deposits contain distinct diatom species, different from the other clastic deposits (Figure 5).

Conversely, clastic deposits 2, 3, 4, and 5 do not match the characteristics discussed above to be classified as tsunami deposits (Table 3). These deposits are all far thinner than deposits 1 and 6 and lack the abrupt, erosional bases that are typical of tsunami deposits (Morton et al., 2007; Switzer and Jones, 2007). They are composed of silt or very fine sand (average d50 between 44 and 78 μm). The lack of any coarse grains is indicative of a lower energy event. We would expect to see larger grain sizes if these units were deposited by a local Alaska-Aleutian subduction zone tsunami, especially since we know larger material is available and was picked up by clastic deposits 1 and 6. We could not identify any grading patterns within these units. The diatom assemblages of

deposits 2, 3 and 4 are mixed and increase in brackish and marine species compared to surrounding peat, but the increases in epipsammic and marine are not as drastic as in deposits 1 and 6 (10-15%). The diatom assemblage of clastic deposit 5 remains mostly freshwater dominated. We do not expect to see drastically different diatom assemblages than the tsunami deposits because the grains are primarily coming from the same source. However, these four deposits all cluster together in the DCA plot, indicating similar species composition, and plot away from clastic deposits 1 and 6. Moreover, there is no paleoseismic record of any other megathrust earthquakes that ruptured this section of the Alaska-Aleutian subduction zone in the time period (Shennan et al., 2014; Gilpin, 1995; Briggs et al., 2014). Based on their lithology and diatom assemblages, we interpret clastic deposits 2, 3, 4, 5 deposits to be either storm deposits, flood deposits, or far field tsunami deposits.

Diatom fracture counts from throughout the core showed only slight variances in percentage of fractured diatom valves between the peat units and the clastic units (differences of <10%). This result is likely because our clastic units contain primarily *Cocconeis* and *Planothidium* diatom species which do not fracture as easily as other species (Witter et al., 2009). The higher percentage of fractured diatoms in classic deposits 1, 2, 3, and 6 may indicate that these deposits were results of higher energy depositional mechanisms (tsunami or storm versus floods) than clastic deposits 4 and 5 (Witter et al., 2009; Nelson et al., 2015; Cooper et al., 2010). Furthermore, we were unable to use the fracture counts as distinctive tsunami deposit indicators.

Using all of our lines evidence, we tried to deduce which type of non-Alaska-Aleutian megathrust earthquake event deposited clastic deposits 2, 3, 4, and 5. Clastic deposit 5 is thin (1.5 cm), fairly fine grained, remains dominated by freshwater, epipelic, and epiphytic diatoms, and contains a slightly lower percentage of fractured valves. Therefore, we expect that this deposit was the result of a small flooding event in the river channel. Clastic deposits 2, 3, and 4 are all similar in thickness (2-3 cm), made up of primarily silt, and contain a higher percentage of marine diatoms than deposit 5 but a lower percentage than deposits 1 and 6. We expect that they were deposited by either storms or tele-seismic tsunamis, which are both lower energy than megathrust tsunamis but still have the ability to bring in marine diatoms (Switzer and Jones, 2008; Kortekaas and Dawson, 2007). Past megathrust earthquakes originating in Japan, including the 2011 Tohuku Earthquake, have sent tele-seismic tsunamis to the coast of Alaska (Heidarzadeh and Satake, 2013). However, it is difficult to match our results with specific historical events.

5.2 Comparison to earthquake records at nearby sites

Previous paleoseismic studies in the Kodiak Island region found evidence of up to six tsunami deposits in marsh stratigraphy dating back to 2200 y BP (Briggs et al., 2014; Shennan et al., 2014; Gilpin, 1995), including the AD 1964 and AD 1788 events. A comprehensive study that covered all of Kodiak Island by Gilpin (1995) found stratigraphic evidence of three paleo earthquakes (either individual events, or clusters) from ~500 yBP, ~800 yBP, and ~1300 yBP, but could not determine whether or not land-

level changes were associated with these events. Gilpin identified one younger tsunami deposit but was unable to determine if it was deposited by the AD 1964 tsunami or the AD 1788 tsunami. Shennan et al. (2014) found a clastic deposit on southeast Kodiak Island of the ~500 yBP event reported by Gilpin, which they dated at AD 1440-1620. Briggs et al. (2014) found a thin tsunami deposit and evidence of land-level change on Sitkinak (15 km southwest of Kodiak Island), which they dated at AD 1430-1650. Both studies found evidence of events from AD 1964 and AD 1788; Briggs et al. (2014) reported uplift associated with the AD 1788 event on Sitkinak and Shennan et al. (2014) reported subsidence on Kodiak.

Based on these previous studies, written records, and eyewitness accounts, we expected to see evidence of two earthquakes and/or tsunamis from AD 1964 and AD 1788 at our site in south central Kodiak Island. Radiocarbon dating indicated that our record at Old Harbor did not extend long enough to record the ~500 yBP event. We know that the AD 1964 tsunami completely inundated Old Harbor with tsunami run-up heights of several meters from various eyewitnesses (Plafker, 1969; Plafker and Khachadoorian, 1966) and thus expected the AD 1964 deposit to be large. We also anticipated the AD 1788 deposit to be a sizable deposit given Old Harbor's proximity to Three Saints Bay (15 km southeast), where at least one large earthquake (with reported subsidence) and a tsunami in the summer of AD 1788 were documented (Soloviev, 1990). The two deposits we identified at our site for these events are both greater than 10 cm thick.

Developing a chronology and a reliable age-depth model for core BC.15.02 was challenging because we were limited by a lack of precise age markers extending beyond

AD 1912. We have only two precise ages in core BC.15.02, the ^{137}Cs peak and the Katmai tephra deposit. Due to the lack of other commonly used chronologic markers such as pollution history (e.g., Kemp et al., 2017; Gerlach et al., 2017), we relied on radiocarbon dating of identifiable plant macrofossils to date the sediments below the tephra deposit. However, because our stratigraphic record at Big Creek is relatively young, the radiocarbon dates are difficult to decipher (Figure 6). Samples from AD 1650-1950 fall within the radiocarbon "modern plateau," which produces multiple calibrated age ranges for each sample, making it nearly impossible to distinguish dates that fall in that time period (Stuiver and Pearson, 1993). Because of these constraints, the Bchron age-depth model had difficulty constraining ages in the deeper section of the core because of the multiple calibrated age ranges for our radiocarbon dates. We were also limited by only having one date from below clastic deposit 6. Therefore, our age model may not predict accurate ages of deposition for each of the clastic deposits. The age model predicts deposition of clastic deposit 6 to be 239-278 yBP, too old to be the AD 1788 event (Figure 7). However, if we look solely at the calibrated age ranges for the sample below clastic deposit 6, one of the age ranges is AD 1780-1800 (Table 1). Such a maximum range would be compatible with this being a tsunami deposit from AD 1788. This evidence, coupled to the strong evidence from the diatoms and the grain-size data, support our interpretation that this is the tsunami from the AD 1788 earthquake.

5.3 Land-level change

Old Harbor lies in the region that subsided during the AD 1964 earthquake. Plafker and Khachadoorian (1966) reported 0.6-0.9 m of subsidence at Old Harbor, which includes sediment compaction. However, we do not see a significant land level change signature in our AD 1964 deposit based on our diatom results. The switch from a freshwater diatom assemblage to a marine assemblage at the base of the AD 1964 deposit to the peat above the sand is not abrupt enough (increase in marine diatoms by 3%, decrease in brackish diatoms by 13%, and percentage of freshwater diatoms remains the same) to indicate a significant positive relative sea-level tendency associated with coseismic subsidence (Figure 4; Nelson et al., 1996; Shennan et al., 2007). Old Harbor lies near the inflection point for coseismic subsidence and uplift for the AD 1964 event, which could be why our results do not indicate any drastic land-level change. Additionally, geodetic surveying data from Ichnose et al. (2007) reports that their nearest site to Old Harbor, on Sitkalidak Island, experienced ~21 cm of subsidence, and subsidence at Old Harbor was most likely just slightly higher. Shennan et al. (2014) reported net subsidence, ~0.35 m, from the AD 1788 earthquake, which is significantly less than what was reported on northern Kodiak Island from the AD 1964 event (1.2-1.5 m). This location may explain why we also did not see a strong subsidence signal associated with our AD 1788 deposit. Comparing the peat above and below the AD 1788 deposit, the diatom assemblages increase in marine by ~8%, increase in brackish by ~6%, and decrease in freshwater species by ~14%, which suggests little to no subsidence (Figure 4). Our site is just north of Sitkinak, which lies over the trench and is where

Briggs et al. (2014) reported coseismic uplift, indicating that Old Harbor lies just away from the trench might explain why we do not see evidence of significant land-level change. However, in order to confirm whether or not our site recorded land-level change and to quantify any possible changes, we would need to apply either a transfer function or another statistical method (Dura et al., 2015; Shennan and Hamilton, 2006; Hemphill-Haley, 1995).

6. Conclusions

We investigated the seismic history (last ~300 years) of south-central Kodiak Island, Alaska by examining salt marsh sediments from Big Creek in Old Harbor. We performed stratigraphic, grain-size, and diatom analyses on a 90 cm core and used our results from these analyses to help us determine whether or not the six clastic layers in our core were deposited by Alaska-Aleutian megathrust earthquakes. Radiocarbon, radiometric, and tephra dating techniques allowed us to associate the deposits in our core with known events from eyewitness accounts, historical reports, and paleoseismic studies from nearby sites.

We identified evidence of two earthquake and associated tsunami events in Old Harbor on Kodiak Island, AK, one from AD 1964 and one that is most likely from AD 1788. Deposits from both of these events were found at nearby sites on Kodiak Island and Sitkinak Island. Grain-size and diatom assemblage results were particularly helpful in helping us distinguish the two tsunami deposits from the other four clastic deposits, which we concluded were deposited by either storms, floods, or tele-seismic tsunamis. The tsunami deposits were thick (>10 cm), contained a wider range of grain sizes (coarser material) with normally graded sequences, and contained a higher percentage of marine and epipsammic diatoms. Results from detrended correspondence analysis on our diatom assemblages showed a clear separation between the local tsunami deposits and the clastic layers from other depositional mechanisms, indicating that DCA is a valuable tool in distinguishing sources of clastic deposits. Our diatom results suggest that little to no land-level change occurred in association with either the AD 1964 or AD 1788 deposits,

which previous studies and eyewitnesses reported. However, to verify whether or not we see a land-level change at Old Harbor, we must apply either a transfer function or another statistical method to our diatom results.

APPENDIX

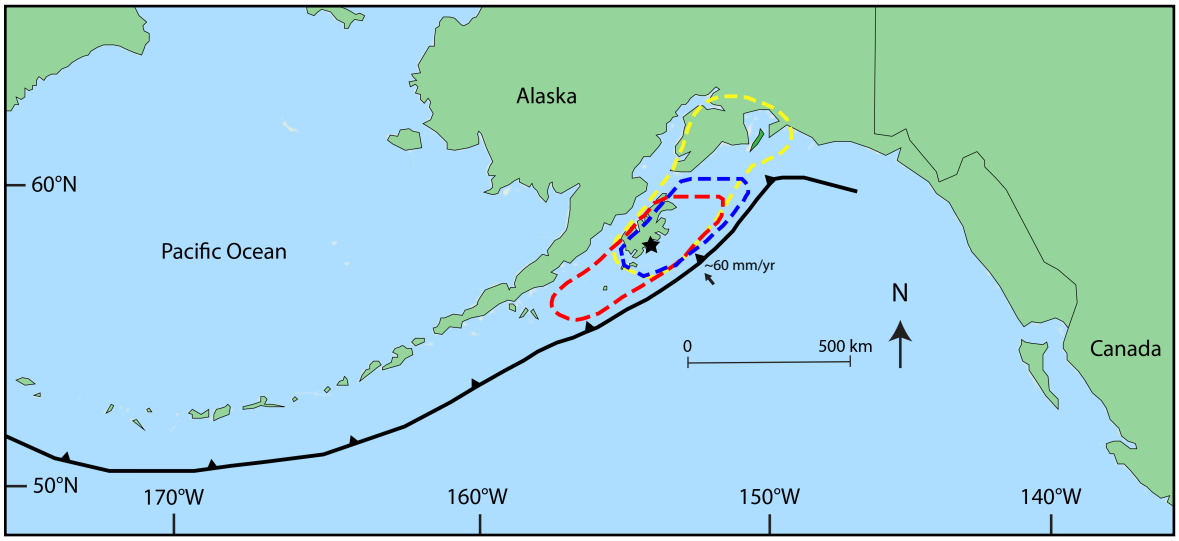

Figure 1. Map of the Alaska-Aleutian subduction zone with the estimated rupture patches of the AD 1964 earthquake (yellow), the AD 1788 earthquake (red), and the ~500 yr BP earthquake (blue) from Shennan et al. (2014) and Briggs et al. (2014) and Plafker (1969). Star indicates our study site, Old Harbor.

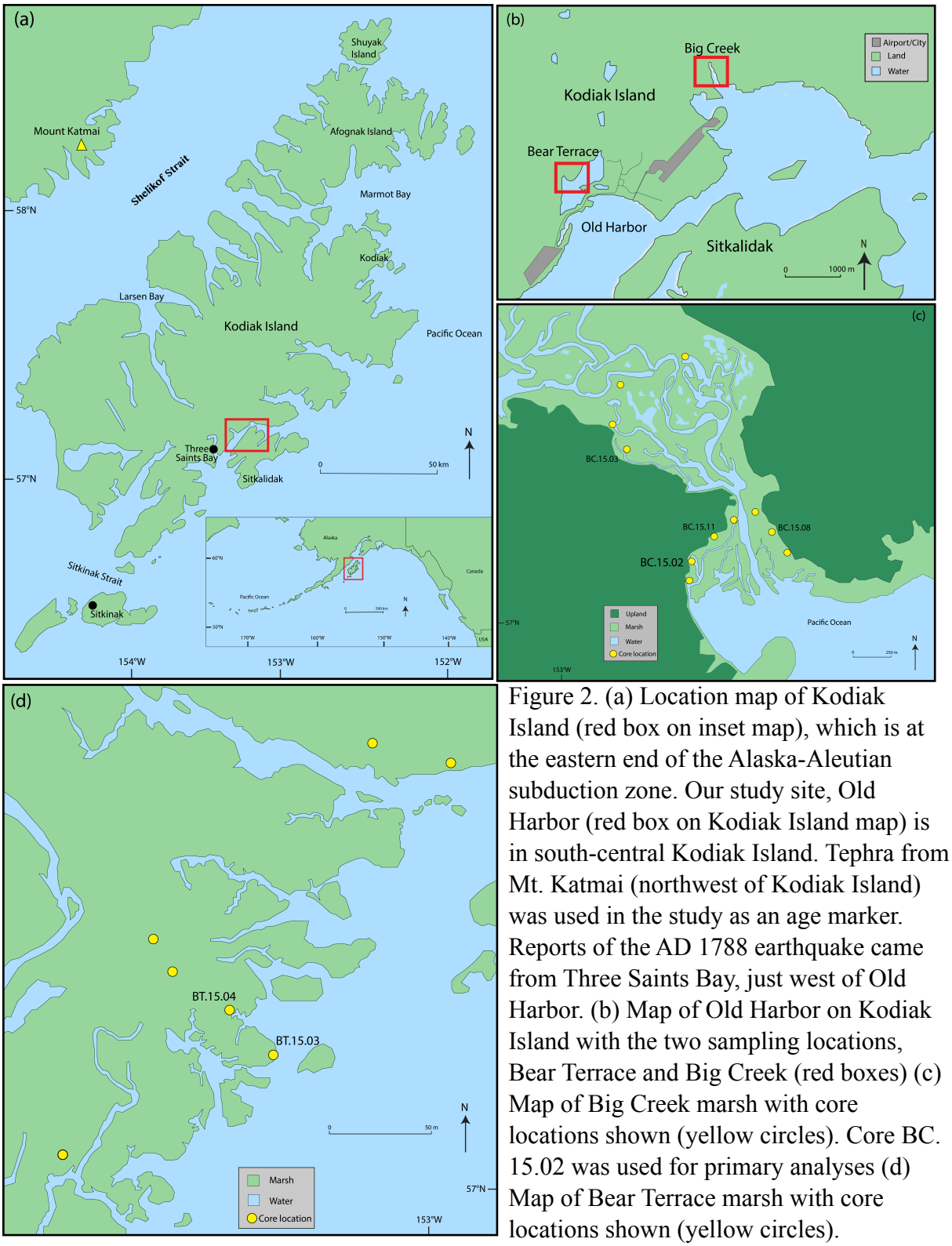

Figure 2. (a) Location map of Kodiak Island (red box on inset map), which is at the eastern end of the Alaska-Aleutian subduction zone. Our study site, Old Harbor (red box on Kodiak Island map) is in south-central Kodiak Island. Tephra from Mt. Katmai (northwest of Kodiak Island) was used in the study as an age marker. Reports of the AD 1788 earthquake came from Three Saints Bay, just west of Old Harbor. (b) Map of Old Harbor on Kodiak Island with the two sampling locations, Bear Terrace and Big Creek (red boxes) (c) Map of Big Creek marsh with core locations shown (yellow circles). Core BC. 15.02 was used for primary analyses (d) Map of Bear Terrace marsh with core locations shown (yellow circles).

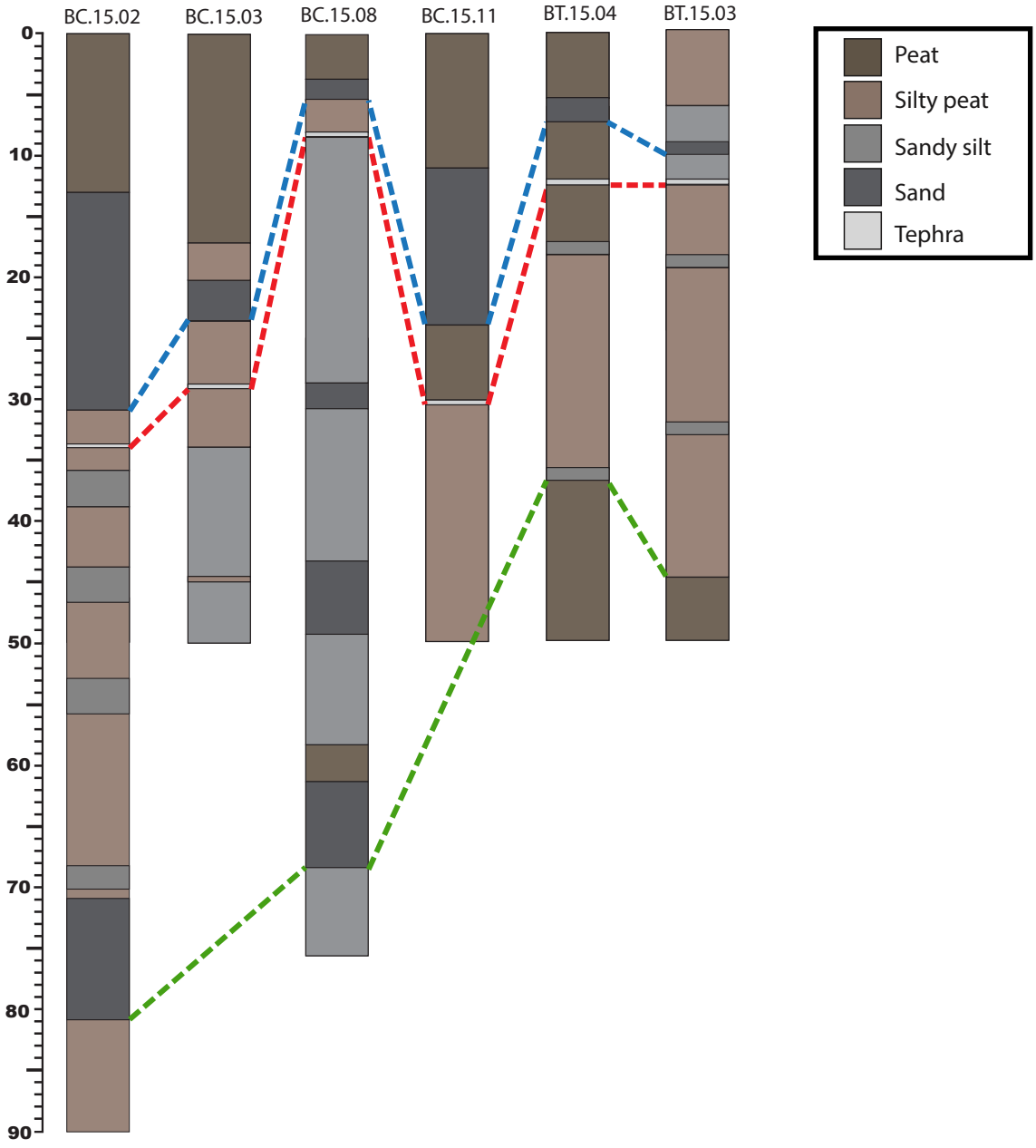

Figure 3. Simplified stratigraphy of selected cores from Big Creek and Bear Terrace. Blue dashed lines correlate the base of the uppermost clastic deposit in each sediment core, red dashed lines correlate tephra deposits from the AD 1912 eruption of Mount Katmai, and green dashed lines correlate the base of the bottommost clastic deposit in the cores.

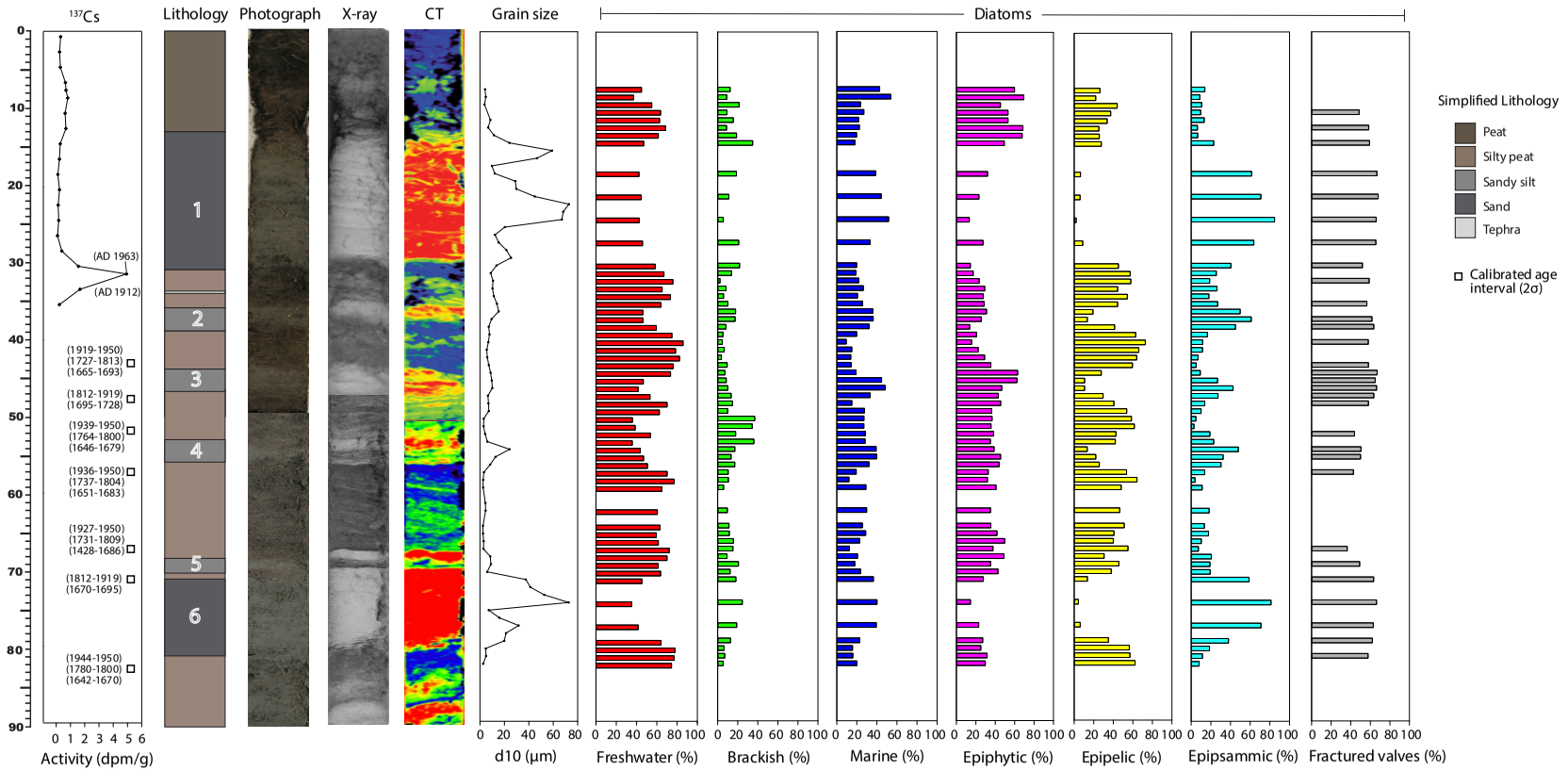

Figure 4. Core BC.15.02 showing (from left to right) ^{137}Cs activity depth profile with calibrated radiocarbon age intervals, simplified lithology, photograph, X-ray image (light gray/white = denser material; dark gray = less dense), CT image (red and orange = denser; blue and green = less dense), grain-size (d10), diatom assemblages as percentages of total valves counted per sample (classified by salinity preference and life-form), and percentage of fractured diatom valves over 40 µm per sample.

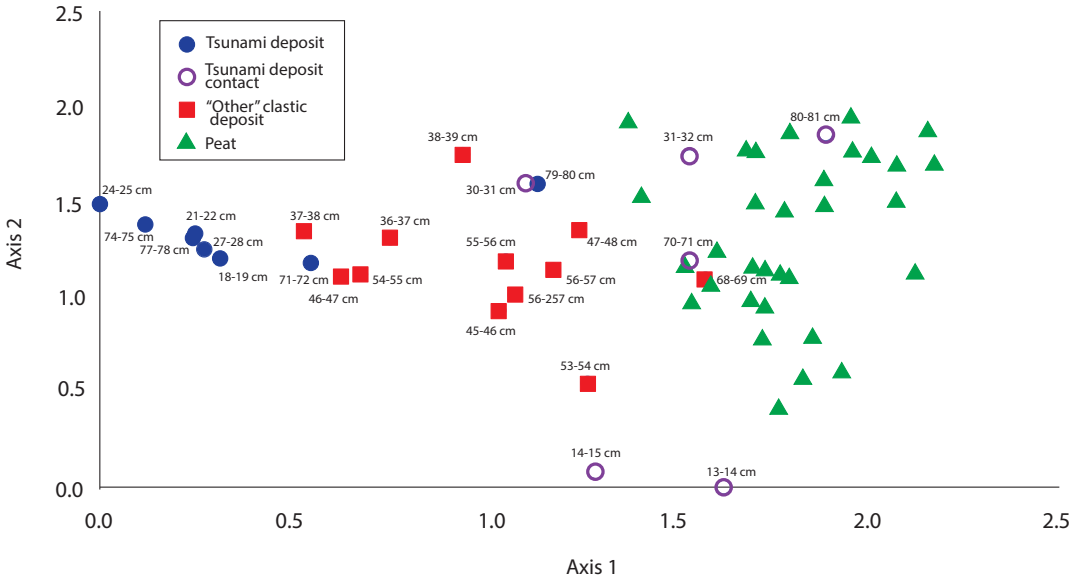

Figure 5. Detrended Correspondence Analysis (DCA) plot of diatom assemblages from samples throughout core BC.15.02. Results show three distinct clusters of samples: tsunami deposit samples (blue circle), clastic deposit samples from other depositional mechanisms (red square), and peat samples (green triangle). Samples from the contacts of the tsunami deposits plotted closer to the peat cluster.

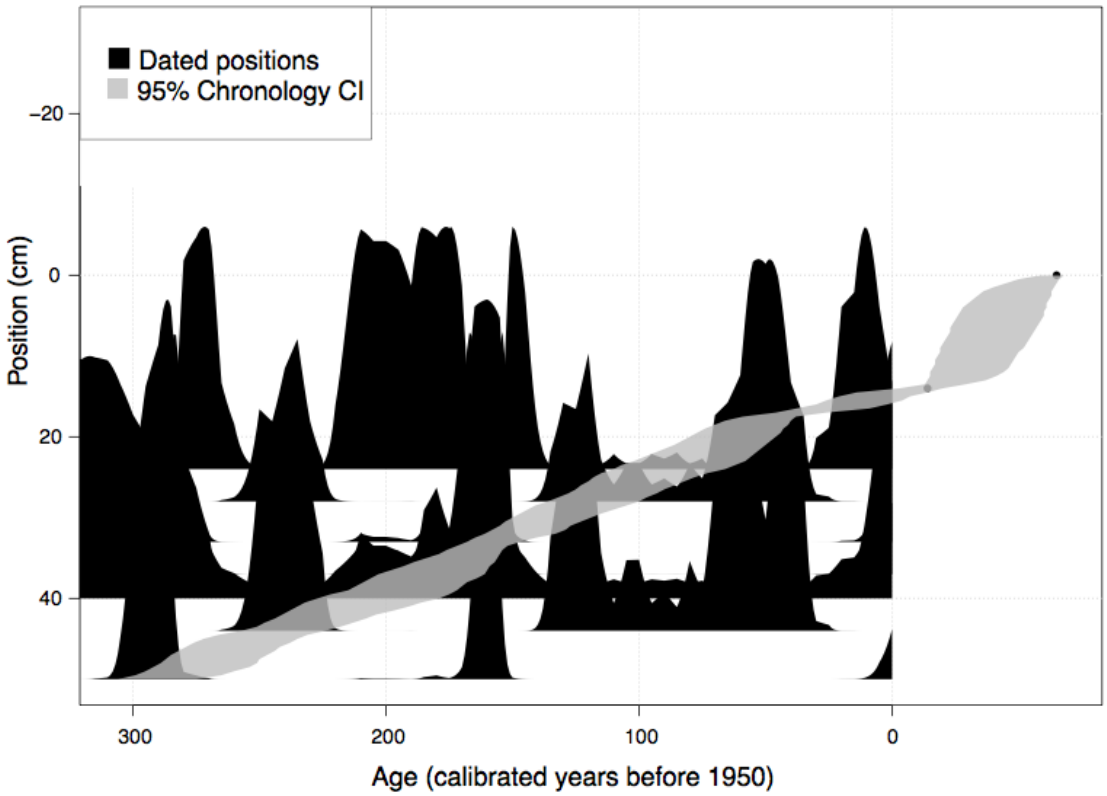

Figure 6. Bchron age-depth model developed for core BC.15.02 with instantaneous clastic deposits removed, showing the 95% probability curve.

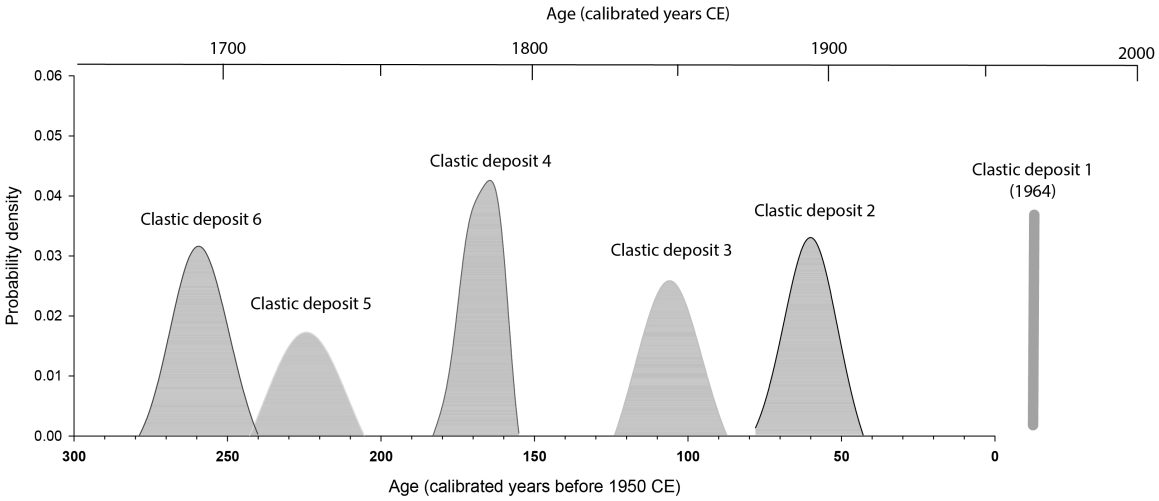

Figure 7. Estimated ages of each of the clastic deposits in core BC.15.02 using our Bchron age-depth model.

Depth (cm)	Sample ID	^{14}C Age (yr BP)	Calibrated age interval (2σ) (yr CE)
43.0	OS-134253	170 ± 20	1919–1950 1727-1813 1665-1693
50.0	OS-134112	75 ± 20	1812–1919 1695-1728
54.5	OS-134182	220 ± 20	1939–1950 1764-1800 1646-1679
62.0	OS-134326	205 ± 20	1936-1950 1737–1804 1651-1683
64.5	OS-134237	315 ± 85	1927-1950 1731-1809 1428-1686
69.5	OS-134113	90 ± 15	1812–1919 1695-1728
87.0	OS-134114	235 ± 20	1944-1950 1780-1800 1642-1670

Table 1. Radiocarbon ages reported by the National Ocean Sciences Accelerator Mass Spectrometry facility and calibrated age intervals from core BC.15.02. Age distributions in gray have been ruled out because of tephra and ^{137}Cs age markers.

Depth (cm)	^{137}Cs activity (dpm/g)	Error
2.50	0.31	0.15
4.50	0.24	0.15
6.50	0.29	0.15
8.50	0.65	0.15
9.50	0.69	0.24
10.50	0.81	0.15
12.50	0.62	0.15
14.50	0.68	0.15
16.50	0.28	0.15
18.50	0.23	0.15
20.50	0.11	0.15
22.50	0.23	0.15
24.50	0.14	0.15
26.50	0.18	0.15
28.50	0.10	0.15
30.50	0.39	0.15
32.50	1.56	0.29
33.50	4.94	0.89
35.50	1.67	0.33
37.50	0.23	0.19

Table 2. Downcore concentrations of ^{137}Cs activity in core BC.15.02 used to determine age markers during the last ~60 years.

	Thickness (>10 cm)	Relatively coarse grained	Wide range of grain sizes	Normally-graded sequences	Mixed diatom assemblage w/ increase in marine &	Abrupt lower contact
Clastic deposit 1	✓	✓	✓	✓	✓	✓
Clastic deposit 2					✓	✓
Clastic deposit 3					✓	
Clastic deposit 4		✓	✓		✓	✓
Clastic deposit 5						
Clastic deposit 6	✓	✓	✓	✓	✓	✓

Table 3. Tsunami deposit characteristic checklist. Black check marks indicate that the deposit met that criteria, gray check marks indicate that the deposit only partially met criteria.

BIBLIOGRAPHY

Barlow, N.L.M., Shennan, I., Long A.J. (2012), Relative sea-level response to Little Ice Age ice mass change in south central Alaska; reconciling model predictions and geological evidence. *Earth and Planetary Science Letters*, 315-316, p. 62-75.

Bourgeois, J. (2009), Geologic effects and records of tsunamis. Chapter 3 in *The Sea*, volume 15, Tsunamis, Harvard University Press, p. 55-91.

Briggs, R. W., S. E. Engelhart, A. R. Nelson, T. Dura, A. C. Kemp, P. J. Haeussler, D. R. Corbett, S. J. Angster, and L.A. Bradley (2014), Uplift and subsidence reveal a nonpersistent megathrust rupture boundary (Sitkinak Island, Alaska). *Geophysical Research Letters*, 41, 2289–2296.

Butler, R., (2012), Re-examination of the potential for great earthquakes along the Aleutian Island arc with implications for tsunamis in Hawaii. *Seismological Research Letters*, v. 83, p. 29-38.

Butler, R., D. Burney, and D. Walsh (2014), Paleotsunami evidence on Kaua'i and numerical modeling of a great Aleutian tsunami. *Geophysical Research Letters*, 41, 6795–6802, doi: 10.1002/2014GL061232.

Butler, R., Walsh, D. & Richards, K. (2017), Extreme tsunami inundation in Hawai'i from Aleutian–Alaska subduction zone earthquakes. *Natural Hazards* 85: 1591. doi:10.1007/s11069-016-2650-0.

Capps, S.R., (1934), Kodiak and Vicinity Alaska. *U.S. Department of the Interior: Mineral Resources of Alaska,* bulletin 868, p. 93-134.

Carter M., Moghissi A. (1977), Three decades of nuclear testing. *Health Physics* 33:55-71.

Carver, G., Plafker, G. (2008), Paleoseismicity and Neotectonics of the Aleutian subduction zone - an overview. *Active Tectonics and Seismic Potential of Alaska: American Geophysical Union*, v. 86, p. 3821-3855.

Combellick, R.A., (1994), Investigation of peat stratigraphy in tidal marshes along Cook Inlet, Alaska, to determine the frequency of 1964 style great earthquakes in the Anchorage region. Alaska Division of Geological and Geophysical Surveys Report of Investigations 94-7, 1-24.

Cooper, S., Gaiser, E., and Wachnicka, A., (2010), Estuarine paleoenvironmental reconstructions using diatoms, in Smol, J.P., and Stoermer, E.F., eds., *The*

diatoms: Applications for the environmental and earth sciences (second edition): Cambridge, U.K., Cambridge University Press, p. 324–345, doi:10.1017/CBO9780511763175.

Corbett DR, Walsh JP and Marciniak K (2009) Temporal and Spatial Variability in the Trace Metals of Two Adjacent Tributaries of the Neuse River Estuary, NC. *Marine Pollution Bulletin* 58(11): 1739-1747.

Dawson, S., Smith, D.E., Ruffman, A., Shi, S. (1996), The diatom biostratigraphy of tsunami sediments: examples from recent and middle Holocene events. Phys. Chem. Earth, v. 21, p. 87-92.

Dawson, A.G., Stewart, I. (2007), Tsunami deposits in the geological record. Sedimentary Geology, v. 200. p. 166-183.

Denys, L., 1991, A checklist of the diatoms in the Holocene deposits of the western Belgian coastal plain with a survey of their apparent ecological requirements I: Introduction, ecological code and complete list: Ministère des affaires économiques. Service Géologique de Belgique, Professional Paper 246, 41.

Diatoms of the United States, (2017). Retrieved from https://westerndiatoms.colorado.edu.

Dura, T., Engelhart, S.E., Vacchi, M., Horton, B.P., Kopp, R.E., Peltier, W.R., Bradley, S., (2016), The role of Holocene relative sea-level change in preserving records of subduction zone earthquakes. *Current Climate Change Reports*, v. 2 p. 86-100.

Dura, T., Hemphill-Haley, E., Y. Sawai, Horton, B.P. (2015), The application of diatoms to reconstruct the history of subduction zone earthquakes and tsunamis. *Earth-Science Reviews*, 152: 181-197.

Dura, T., Cisternas, M., Horton, B.P., Ely, L.L., Nelson, A.R., Wesson, R.L., Pilarczyk, J.E. (2015b), Coastal evidence for Holocene subduction-zone earthquakes and tsunami in central Chile. *Quaternary Science Reviews,* v. 113, p. 93-111.

Fierstein, J., Hildreth, W. (1992), The plinian eruptions of 1912 at Novarupta, Katmai National Park, Alaska. *Bulletin of Volcanology* 54: 646-686.

Folk, R.L., (1966), A review of grain-size parameters. *Sedimentology* 6: 73-93.

Fujino S., Masuda, F., Tagomori., S., Matsumoto, D. (2006), Structure and Depositional process of a gravelly tsunami deposit in a shallow marine setting: Lower Cretaceous Miyako Group, Japan. *Sedimentary Geology* 187: 127-138.

Gerlach M.J., Engelhart S.E., Kemp AC et al. (2017), Reconstructing Common Era relative sea-level change on the Gulf Coast of Florida. *Marine Geology* 390: 254-269.

Gilpin, L.M., (1995), Holocene paleoseismicity and coastal tectonics of the Kodiak Islands, Alaska. Ph.D. dissertation, 358, Univ. of California Santa Cruz, Santa Cruz, California.

Hamilton, S., Shennan, I. (2005a), Late Holocene relative sea-level changes and the earthquake deformation cycle around upper Cook Inlet, Alaska. *Quaternary Science Reviews,* v. 24, p. 1479-1498.

Hamilton, S., Shennan, I., Combellick, R., Mulholland, J., Noble, C. (2005b), Evidence for two great earthquakes at Anchorage, Alaska and implications for multiple great earthquakes through the Holocene. *Quaternary Science Reviews,* 24: 2050-2068.

Haslett, J. and Parnell, A., 2008. A simple monotone process with application to radiocarbon‐dated depth chronologies. *Journal of the Royal Statistical Society: Series C (Applied Statistics)*, *57*(4), p. 399-418.

Heidarzadeh, M. And Satake, K., 2013. Waveform and Spectral Analyses of the 2011 Japan Tsunami Records on Tide Gauge and DART Stations Across the Pacific Ocean. *Pure and Applied Geophysics,* 170, p. 1275-1293.

Hemphill-Haley. E. (1993), Taxonomy of recent and fossil (Holocene) diatoms (Bacillariophyta) from northern Willapa Bay, Washington. U.S. Department of the Interior: U.S. Geological Survey, Open-File Report, 93-289.

Hemphill-Haley, E. (1995), Diatoms as evidence for earthquake-induced subsidence and tsunami 300 yr ago in southern coastal Washington. *Geological Society of America Bulletin,* v. 107, p. 367-378.

Hemphill-Haley, E. (1996), Diatoms as an aid in identifying late-Holocene tsunami deposits. *The Holocene* 6,4, p. 439-448.

Horton B.P., and Edwards R.J. (2006), Quantifying Holocene Sea Level Change using Intertidal Foraminifera: Lessons from the British Isles. Cushman Foundation for Foraminiferal Research, Special Publication, Volume 40: 97. Retrieved from http://repository.upenn.edu/ees_papers/50.

Hong, I., Dura, T., Ely, L.L., Horton, B.P., Nelson, A.R., Cisternas, M., Nikitina, D., Wesson, R.L. (2016), A 600-year-long stratigraphic record of tsunami in south-central Chile. *The Holocene*, v. 27, p. 39-51.

Kachadoorian, Reuben and George Plafker, Effects of the Earthquake of March 27, 1964 on the Communities of Kodiak and Nearby Islands. U.S. Geological Survey Professional Paper 542-F, 41.

Kemp A.C., Hill T.D., Vane CH et al. (2017), Relative sea-level trends in New York City during the past 1500 years. *The Holocene* 1-18, DOI: 10.1177/0959683616683263.

Kirby, S., Scholl, D., von Huene, R., Wells, R., (2013), Alaska earthquake source for the SAFRR Tsunami Scenario. U.S. Geological Survey Open-File Report 2013-1170-B.

Kortekaas, S., Dawson, A.G. (2007), Distinguishing tsunami and storm deposits: an example from Martinhal, SW Portugal. *Sedimentary Geology* 200:208-221.

Krammer, K., and Lange-Bertalot, H., (1986), Bacillarophyceae 1. Teil Naviculaceae: Süßwasserflora von Mitteleuropa, Band 2/1: Stuttgart, Gustav Fischer Verlag, 876.

Krammer, K., and Lange-Bertalot, H., 1988, Bacillarophyceae 2. Teil Basillariaceae, Epithemiaceae, Surirellaceae: Süßwasserflora von Mitteleuropa Band 2/2: Stuttgart, Gustav Fischer Verlag, 600.

Krammer, K., and Lange-Bertalot, H., 1991a, Bacillarophyceae 3. Teil Centrales, Fragilariaceae, Eunotiaceae: Süßwasserflora von Mitteleuropa Band 2/3: Stuttgart, Gustav Fischer Verlag, 600.

Krammer, K., and Lange-Bertalot, H., 1991b, Bacillarophyceae 4. Achnanthaceae, Kritische Erganzungen zu Navicula (Lineolatae) und Gomphonema: Süßwasserflora von Mitteleuropa Band 2/4: Stuttgart, Gustav Fischer Verlag, 437.

Morton, R.A., Gelfenbaum, G., Jaffe, B.E. (2007), Physical criteria for distinguishing sandy tsunami and storm deposits using modern samples. Sedimentary Geology (200), p. 184-207.

Nanayama, F., Furukawa, R., Shigeno, K., Makino, A., Soeda, Y., Igarashi, Y. (2007), Nine unusually large tsunami deposits from the past 4000 years at Kiritappu marsh along the southern Kuril Trench. *Sedimentary Geology,* 200, p. 275-294.

National Oceanic and Atmospheric Administration (NOAA), https://tidesandcurrents.noaa.gov/sltrends/sltrends_station.shtml?stnid=9457292.

Nelson, A. R., Shennan, I., and Long A. J. (1996), Identifying coseismic subsidence in tidal-wetland stratigraphic sequences at the Cascadia subduction zone of western North America. J. *Geophysical Research*, 101(B3), 6115-6135.

Nelson, A.R., Briggs, R.W., Dura, T., Engelhart, S.E., Gelfenbaum, G., Bradley, L., Forman, S., Vane, C.H., Kelley, K.A. (2015), Tsunami recurrence in the eastern Alaska-Aleutian arc: A Holocene stratigraphic record from Chirikof Island, Alaska. *Geosphere,* v. 11, no. 4, op. 1172-1203, doi:10.1130/GES01108.1.

Nishenko, S.P., Jacob, K.H., (1990), Seismic potential of the Queen Charlotte-Alaska-Aleutian seismic zone. *Journal of Geophysical Research,* vol. 95, no. B3, p. 2511-2532.

Parnell, A.C., Buck, C.E., Doan, T.K., (2011), A review of statistical chronology models for high-resolution, proxy-based Holocene palaeoenvironmental reconstruction. *Quaternary Science Reviews* 30 2948-2960.

Parnell, A.C., Gehrels, W.R. (2015), Using chronological models in late Holocene sea-level reconstructions from saltmarsh sediments. Handbook of Sea-Level Research, p. 500-513.

Plafker, G. (1969), Tectonics of the March 27, 1964 Alaska Earthquake, Geological Survey Professional Paper 543-I.

Plafker, G., Kachadoorian, R. (1966), Geologic Effects of the March 1964 Earthquake and associated seismic sea waves on Kodiak and nearby islands Alaska. Geological Survey Professional Paper, 543-D.

Reimer P.J., Bard E., Bayliss A. et al. (2013), INTCAL13 and marine13 radiocarbon age calibration curves 0-50,000 years CAL BP. *Radiocarbon 55*(4): 1869-1887.

Ryan, H.F., von Huene, R., Wells, R.E., Scholl, D.W., Kirby, S., and Draut, A.E. (2012), History of earthquakes and tsunamis along the eastern Aleutian-Alaska megathrust, with implications for tsunami hazards in the California Continental Borderland. Studies by the U.S. Geological Survey in Alaska, 2011: U.S. Geological Survey Professional Paper 1795–A, 31.

Sawai, Y. (2001), Distribution of living and dead diatoms in tidal wetlands of northern Japan: relations to taphonomy. *Palaeogeogrphy, Palaeoclimatology, Palaeoecology* 173, 125-141.

Sawai, Y., Fujii, Y., Fujiwara O., Kamataki, T., Komatsubara J., Okamura, Y., Satake, K., Shishikura, M. (2008). Marine incursions of the past 1500 years and evidence of tsunamis at the Suijin-numa, a coastal lake facing the Japan trench. *The Holocene* 18, 517-528.

Shennon, I., Barlow, N., Carver, G., Davies, F., Garret, E., Hocking, E. (2014), Great tsunamigenic earthquakes during the past 1000 yr on the Alaska megathrust. *Geology*, v. 42; no. 8; p. 687-690.

Shennan, I., Barlow, N., Combellick, R., Pierre, K., Stuart-Taylor, O. (2014), Late Holocene paleoseismology of a site in the region of maximum subsidence during the 1964 Mw 9.2 Alaska earthquake. *Journal of Quaternary Science*, 29(4) 343-350.

Shennan, I., Bruhn, R., Barlow, N., Good, K., Hocking, E. (2014), Late Holocene great earthquakes in the eastern part of the Aleutian megathrust. *Quaternary Science Reviews* 84: 86-97.

Shennan, I., Hamilton, S. (2005), Coseismic and pre-seismic subsidence associated with great earthquakes in Alaska. *Quaternary Science Reviews* 25: 1-8.

Shennan, I., Hamilton, S., Long, A. (2003), Late Holocene paleoseismicity and associated land/sea level changes in the greater Anchorage area. Program element II: Research on Earthquake Occurrence and Effect.

Shennan, I., Long, A., Barlow, N. (2007), Recurrent holocene paleoseismicity and associated land/sea level changes in south central Alaska. Alaska Division of Geological and Geophysical Surveys.

Shennon, I., Scott, D. B., Rutherford, M., Zong, Y., (1999), Microfossil analysis of sediments representing the 1964 earthquake, exposed at Girdwood Flats, Alaska, USA. *Quaternary International* 60: 55-73.

Soloviev, S.L., (1990) Sanak-Kodiak tsunami of 1788. Science of Tsunami Hazards, v. 8, p. 34-30.

Stuiver M. and Pearson G.W., (1993) High precision bidecadal calibration of the radiocarbon timescale, AD 1950-500 BC and 2500-6000 BC. *Radiocarbon* 35: 1-23.

Switzer, A.D., and Jones, B.G.,(2008), Large-scale washover sedimentation in a freshwater lagoon from the southeast Australian coast: Sea-level change, tsunami or exceptionally large storm?: *The Holocene*, v. 18, p. 787–803, doi: 10.1177/0959683608089214.

Switzer, A., and Pile, J., (2015), Grain size analysis. Handbook of Sea-Level Research.

Troels-Smith, J., (1955), Karakterisering af lose jordarter. Characterization of unconsolidated sediments.

United States Geological Survey (2014), The 1964 Great Alaska Earthquake and Tsunami, http://earthquake.usgs.gov/earthquakes/events/alaska1964/.

Vos, P.C., and de Wolf, H., (1988), Methodological aspects of paleo-ecological diatom research in coastal areas of the Netherlands. Geologie en Mijnbouw, v. 67, p. 31–40.

Vos, P.C., and de Wolf, H., (1993), Diatoms as a tool for reconstructing sedimentary environments in coastal wetlands; methodological aspects, in von dam, H., ed., Twelfth International Diatom Symposium. Hydrobiologia, v. 269/270, p. 285–296, doi:10.1007/BF00028027.

Witter, R.C., Kelsey, H.M., and Hemphill-Haley, E., (2003), Great Cascadia earthquakes and tsunamis of the past 6700 years, Coquille River estuary, southern coastal Oregon. *Geological Society of America Bulletin*, v. 115, p. 1289–1306, doi:10.1130/B25189.1.

Witter, R.C., Hemphill-Haley, E., Hart, R., and Gay, L., (2009), Tracking prehistoric Cascadia tsunami deposits at Nestucca Bay, Oregon: Final technical report. U.S. Geological Survey, National Earthquake Hazards Reduction Program Award 08HQGR0076, 40 p., http://earthquake.usgs.gov/research/external/reports/08HQGR0076.pdf.

Zong, Y., Shennan, I., Combellick, R.A., Hamilton, S.L., Rutherford, M.M. (2003), Microfossil evidence for land movements associated with the AD 1964 Alaska earthquake. *The Holocene* 13,1, pp. 7-20.